NEW YORK UNIVERSITY
WASHINGTON SQUARE COLLEGE
MATHEMATICS RESEARCH GROUP
RESEARCH REPORT No. EM-12

NOTES ON DIFFRACTION BY A CIRCULAR DISK

by

ALFRED LEITNER

The research reported in this document has been made possible through support and sponsorship extended by the Geophysical Research Directorate of the Cambridge Field Station, AMC, U. S. Air Force, under Contract No. AF 19 (122)-42. It is published for technical information only and does not represent recommendations or conclusions of the sponsoring agency.

APRIL, 1949

New York University
Washington Square College
Mathematics Research Group

Research Report No. EM-12
under
Contract No. AF-19(122)-42

NOTES ON DIFFRACTION BY A CIRCULAR DISK

by

Alfred Leitner

Written by:

Alfred Leitner

Alfred Leitner

Morris Kline

Morris Kline
Project Director

Title page
36 numbered pages

April, 1949

CONTENTS

ABSTRACT

This report investigates diffraction of a plane sound wave from a rigid circular disk of zero thickness. A recently published exact theory is extended to compute and discuss values for the diffracted field both at the disk and at large distances from it. The Kirchhoff solution - an approximation designed for the case of very short wave length - is compared to the exact solution and it is found to be more powerful than might heretofore have been supposed. The reasons for this are discussed in some detail.

1. Introduction

The mathematical techniques employed in solving boundary value problems in diffraction are essentially the same for electromagnetic, or vector, and for acoustic, or scalar, waves. It is reasonable, therefore, to consider them together in a general discussion.

Surprisingly, exact solutions exist for only a rather limited variety of diffracting obstacles. We understand by "exact" solutions those which satisfy the underlying fundamental equations, such as, for example, Maxwell's field equations, subject to the correct boundary conditions. As we shall see, solutions which meet both these conditions still are not necessarily complete, although they would appear to be. For instance, they may be in the form of series known to be convergent, but converging so slowly in certain regions of the frequency parameter that their evaluation in these regions presents an excessive computing problem. Let us call such results "exact in principle". Many valuable conclusions still can be drawn from these, but it may not be feasible to plot, say, radiation patterns for all frequency ranges. We shall be concerned here with a solution of this type to the problem of diffraction by the circular disk.

It is apparently simplest to treat "semi-infinite" scatterers. By that we mean scatterers of such shape that they extend infinitely in one or several directions. As examples we mention the infinite cylinder or the half-plane.

On dealing with finite obstacles, however, such as our disk, or obstacles of shapes closely related thereto, such as the infinite screen with a circular aperture, additional difficulties are encountered which are characteristic of the geometry, especially so in the electromagnetic case. We shall point these out in connection with the disk.

Three essentially different "exact" methods have been employed in this type of problem

One is Sommerfeld's exact solution to the scattering by the half-plane, explicit for all frequencies[1]. This is quite unique and may not be extensible to other geometries.

Another is based on the Wiener-Hopf method of solving integral equations with kernels having special properties. It was recently first applied in diffraction by Schwinger to the problem of the bifurcated wave guide[2]. It is known that any wave problem may be formulated by a partial differential equation - the wave equation - with appropriate boundary conditions, or by an integral equation comprising the boundary conditions. The latter can be obtained by Green's function techniques. If, and only if, the kernel is a function of the difference of its arguments can this method be employed. This limits the variety of scatterers. Among other problems to which the method has been successfully applied are the radiation from a semi-infinite cylinder[3], and the diffraction from two and from an infinite set of parallel half-planes[4].

The third method[5] will be considered in some detail, since it is the one on which our work is based. It is the method of eigenfunctions. The wave function of the scattered field (field vectors or velocity potential, depending upon whether it is the electromagnetic or acoustic problem) is here expressed as a series of eigenfunctions; hence in view of observations above the method is exact only "in principle".

In a vector problem involving divergenceless vectors, e.g., charge free space, the wave functions $\underset{\sim}{V}$ are solutions of

(1) $$-\nabla \times \nabla \times \underset{\sim}{V} + k^2 \underset{\sim}{V} = 0, \quad k = \frac{2\pi}{\lambda},$$

and can be constructed from those solutions of the scalar wave equation

(2) $$\nabla^2 \psi + k^2 \psi = 0$$

which are characteristic of, i.e. eigenfunctions of, the particular geometry of the problem. Thus the two pairs of vectors

(3) $$\nabla \times \underset{\sim}{a} \psi, \quad \nabla \times \nabla \times \underset{\sim}{a} \psi$$

(4) $$\nabla \times \underset{\sim}{r} \psi, \quad \nabla \times \nabla \times \underset{\sim}{r} \psi$$

where ψ is a solution of the scalar wave equation, $\underset{\sim}{a}$ is any constant vector and $\underset{\sim}{r}$ the radius vector, form two different sets of independent solutions to (1). No variable vectors other than $\underset{\sim}{r}$ are known to supply proper vector wave functions. In fact it may not be commonly known that (4) itself is a general solution; it has been used in the discussion of

electromagnetic diffraction by the sphere, solved exactly by Stratton[6], as characteristic of the spherical coordinate system, in which r is a coordinate variable.

The velocity potential in <u>acoustical</u> wave problems is a solution of the scalar wave equation (2) and this proves the point previously made that the two types of problems may be discussed together.

Now, it is possible to separate the space variables in (2) in 11 different orthogonal curvilinear coordinate systems[7]. Such a procedure leads to ordinary second order differential equations of the Sturm-Liouville type. These generate infinite and complete sets of orthogonal eigenfunctions, often known as "special functions". Far from all the sets of functions corresponding to the eleven systems have been analyzed. One of these sets, for example, are the wave functions of the oblate spheroid. The coordinate system consists of oblate spheroids ξ , a circular disk

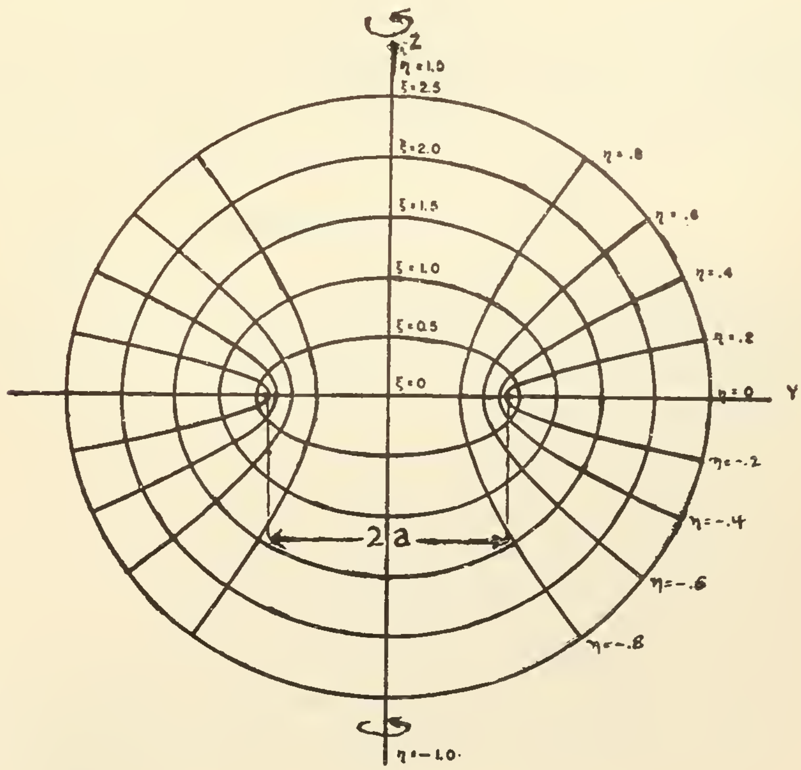

The oblate spheroidal coordinates
Fig. 1

of zero thickness being the limiting spheroid $\xi = 0$, hyperboloids of revolution about z and of one sheet, $\pm\eta$, and planes of constant azimuth ϕ. The oblate spheroidal wave functions have been investigated by a number of authors. Tables have in recent years been compiled by Stratton, Chu, et. al.[8] and considerably extended by Leitner and Spence[9].

Whenever another set of "special" functions is investigated and tabulated, the way is opened for the solution of a number of boundary value problems. For, whenever the boundary of a diffraction problem may be made to coincide with coordinate surfaces of one of these systems, the appropriate wave function Ψ can be expanded easily as a series of the product-eigenfunctions.

With this method a number of diffraction problems has been solved. The results of Sommerfeld were reproduced by Epstein[10] with the half-plane as a limiting parabolic cylinder. The diffraction by infinite slits and strips was investigated by Morse and Rubinstein[11], using the wave functions of the elliptic cylinder.

In the class of finite scatterers of electromagnetic waves we have, first, the work of Stratton[6] on the diffraction by spheres, using the eigenvector functions (4) to generate a given field. The scalar eigenfunctions are of the form

$$\Psi_{\ell m} = z_\ell(kr)\, P_\ell^m(\cos\theta)\, \begin{matrix}\cos\\ \sin\end{matrix}\, m\phi \quad . \tag{5}$$

Here r, θ, ϕ are the spherical coordinates, the functions z_ℓ are the radial spherical wave functions of order ℓ - half-integral-order solutions of Bessel's equation-and the P_ℓ^m are the associated Legendre functions. Note that all these separate functions belong to the class of hypergeometric functions and their so-called confluences. The analysis of this class of functions can be considered as completely known, and their properties as simple relative to other functions arising out of the solution of (2), for example, the wave functions of the oblate spheroid. Thus general recursion formulae between different functions and their derivatives are known, also the generating functions are known in the former cases, but not in the latter example.

These circumstances aid in making the form of the vector solutions relatively simple for the sphere and are reasons for assuring a sort of vectorial-functional orthogonality between functions $\nabla \times \underset{\sim}{r} \psi_{\ell m}$ and $\nabla \times r \psi_{\ell' m'}$ and the like. To this is added significantly the fact that solutions (4) are everywhere transverse to $\underset{\sim}{r}$, a coordinate vector of this particular problem, but not necessarily of others, and these vectors are tangent to the boundaries of the problem.

This is not so in the spheroidal problem of the disk, for example. Apparently no vector solutions are known here which have convenient vector orthogonality properties, essential to problems employing series of such solutions.

A similar difficulty is encountered with the prolate spheroid, which in the limit may be taken as a wire of zero thickness and finite length. This problem was discussed by Page[12] and Ryder[13], for a normally incident plane wave. It is the case of the receiving antenna. Their discussions are limited to resonance effects and a complete diffraction solution is still outstanding.

The difficulty is, however, removed in the scalar case, because functional orthogonality obtains in all of the eleven systems referred to above, in which the wave equation is separable.

We may draw the following conclusions. A number of diffraction problems involving finite geometrical boundaries coincident with a certain group of coordinate surfaces may be attacked by the method of the generalized Fourier series of eigenfunctions. The scalar solution depends on whether the corresponding wave functions have been or can be analyzed. The vector solution is complicated by the fact that we apparently know no method of finding vector eigenfunctions most appropriate to the geometry of the problem. An exact and complete theory exists only for the sphere.

Considering, therefore, the problem of diffraction of electromagnetic waves by the perfectly conducting disk as unsettled, let us turn our attention to the diffraction of sound by the rigid disk. The exact theory for the circular disk, based on the wave functions of the oblate spheroid, was independently formulated by Spence[14] and Bouwkamp[15]. These

authors both consider a monochromatic plane wave at normal incidence, and proceed to compute, from tables of the functions and allied coefficients, the scattering cross section σ as a function of the parameter ka, where a is the radius of the disk. The quantity ka is a measure of the ratio of diameter to wavelength. The quantity σ is defined as the ratio of the total scattered power flow outward to the power flux incident on the scatterer. It is obtained by summing the scattered power flux, usually calculated at large distances, over all directions.

We shall refer to the values of the velocity potential, and its gradient, at large distances as the "distant field". These and the values of quantities derived therefrom - such as σ - are as a rule the results of foremost interest in a diffraction theory.

As a consequence of this a number of methods have been devised whereby the distant field can be calculated approximately, long before exact theories could have been formulated.

Such approximations generally begin by assuming certain conditions at or near the scatterer which are either known, or believed to be incorrect. The assumptions are different in different ranges of ka.

When the value of ka is small - large scatterers - the method of Rayleigh may be applied. The assumption is that conditions near the scatterer, e.g., at distances small compared to λ, are essentially static, k being relatively small in equation (2), while sufficiently far away the diffracted wave from any finite obstacle must be spherically diverging. Thus an <u>approximate</u> distant field is obtained. This was applied to the circular disk by Rayleigh himself[16].

A more powerful method, using variational principles, was very recently applied to the aperture by Levine and Schwinger[17]. It makes possible an approximate calculation of the distant field (scattering cross section) up to values for ka of the order **10.** It is just in this region that the spheroidal solution of Bouwkamp and Spence, when applied to the aperture, conveniently supplies exact results, while at larger values computation would become excessive. Comparison of the several results for σ show excellent agreement. We refer the reader to figure 2 of the paper by Levine and Schwinger.

Finally there exists the method, due to Kirchhoff, of obtaining approximate diffraction formulas at large distances from the scatterer - or aperture - which applies only, or supposedly only, as $ka \to \infty$. It is the method frequently used in physical optics. The problem is actually an electromagnetic one there, but it is reduced to a scalar problem on certain cartesian components of the field vectors. Acoustic diffraction may therefore a fortiori be treated from the Kirchhoff point of view. The method, and its limitations in the general case, are discussed by Baker and Copson[18]. However we shall see in this paper that this method is quite powerful in certain problems - namely those dealing with obstacles lying entirely in a plane - more powerful than might heretofore have been supposed. In other words, we will show that the method produces good approximations for the distant field even at relatively small values of ka.

The assumptions made are confined to the values of the function at the boundary. For, the wave field at a point P inside a closed surface S is given exactly by the Helmholtz formula[19],

$$(6) \qquad \psi(P) = \frac{1}{4\pi} \iint_S \left[\frac{\partial \psi}{\partial n} \frac{e^{ikR}}{R} - \psi \frac{\partial}{\partial n} \left(\frac{e^{ikR}}{R} \right) \right] ds,$$

in terms of the values on S of ψ and its derivative along the outward normal $\underset{\sim}{n}$, if all singularities of ψ are exterior to S. Here R is the distance from points on S to the point P. The boundary values are now usually taken such that on the parts of S occupied by the obstacle there is a complete shadow on the surface of the obstacle not exposed to the incident wave, perfect reflection on the exposed side, and a vanishing diffraction effect in the plane of the obstacle, if it lies in a plane. In view of our knowledge based on phenomena in optics, dealing with very short λ, these are reasonable assumptions.

In the following sections it will be shown rigorously that the last mentioned of the above Kirchhoff assumptions for plane obstacles are not approximative, but exact. We will also present the Kirchhoff

solution for the rigid disk* in acoustic diffraction, in order to compare it with results of the exact solution.

In addition we will extend the results of the exact spheroidal theory of Bouwkamp and Spence. Thus we will obtain the radiation pattern, which is defined as the scattered outward power flux at infinity as a function of direction, at a set of ka values, ka $\leq$ 5 and compare these with the corresponding Kirchhoff curves.

It is of considerable interest to know also the exact conditions on the surface of the disk. First of all, one would like to appraise the approximative Kirchhoff assumptions on the surface of a scatterer. Secondly no exact theory for values in this region exist for any finite scatterer beside the sphere. It is for just these reasons that, very recently, F. M. Wiener made experimental acoustic measurements on rigid spheres and cylinders[21], rigid circular and square disks[22]. The spheroidal theory permits a study of conditions on the disk and this will form a part of our discussions from which a number of conclusions can be drawn and the experimental data can be evaluated.

---

* A Kirchhoff treatment yielding values for the field at points near the axis of symmetry of the disk is also found in a paper by Primakoff, et al[20].

2. Approximate Solution by the Kirchhoff Method

The Kirchhoff boundary conditions are as follows: the disk acts as if it were a perfect reflector of infinite size. For the incident field we take a normally incident plane wave of unit amplitude coming from z = + ∞ and progressing in the negative z direction. We may then, place our disk of zero thickness in the plane z = 0. The incident velocity potential is

(7) $$\Psi_{inc} = e^{-ikz} .^{*}$$

The scattered velocity potential will be denoted by Ψ_s, and an additional subscript K will be used whenever we speak of a value obtained by, or assumed in, the Kirchhoff theory. On the positive side of the disk the total field is doubled by the Kirchhoff assumption of perfect reflection, $\Psi_{s,K} = \Psi_{inc}$; on the negative side a shadow is assumed to exist, $\Psi_{s,K} = -\Psi_{inc}$; in the remaining portion of z = 0 we must take $\Psi_{s,K} = 0$. These conditions are expressed in figure 2.

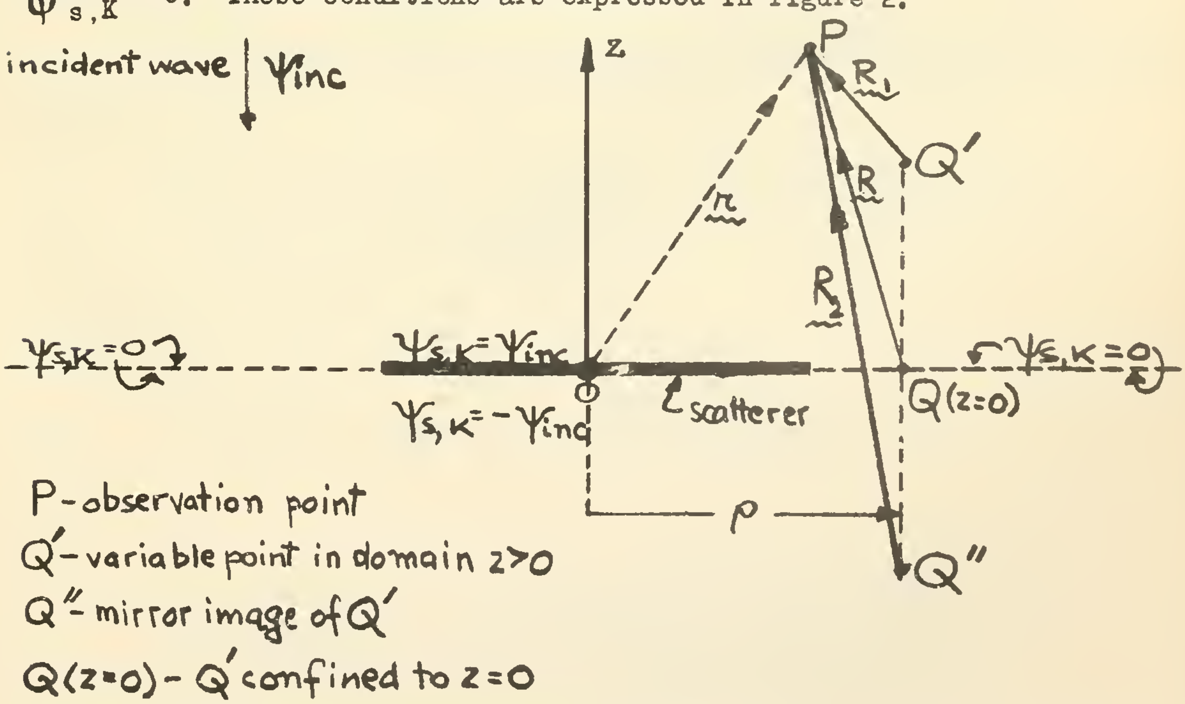

Scatterer lying in the xy-plane. For discussion, see pages 10, 14 and 24.
Fig. 2

---

* time dependence $e^{-i\omega t}$ removed.

We will not show here how the Helmholtz integral (6) can be reduced in our type of problem, which deals with two semi-infinite regions separated by a surface (the plane $z = 0$). The arguments are found in the texts[23]. We state here merely that, if ψ_s satisfies the Sommerfeld conditions

$$(8) \qquad r\,\psi_s < N\,, \quad r\left(\frac{\partial \psi_s}{\partial r} - ik\,\psi_s\right) = 0 \quad \text{as } r \to \infty\,,$$

where N is some finite number and r is the radius vector from the origin, then

$$(9) \qquad \psi_s(P) = -\frac{1}{2\pi} \iint_{(z=0)} \psi_s \frac{\partial}{\partial n}\left(\frac{e^{ik|\underset{\sim}{r} - \underset{\sim}{\rho}|}}{|\underset{\sim}{r} - \underset{\sim}{\rho}|}\right) dx\,dy$$

where r is the distance from the origin to P and ρ the distance from the origin to any point Q on $z = 0$, cf. figure 2. Conditions (8) are general conditions which ensure that the scattered wave function and its radial derivative behave like spherically diverging waves, e.g. have a radial dependence $\frac{e^{ikr}}{r}$, at large r.

Under the Kirchhoff assumptions for a plane obstacle the integral takes the form

$$(10) \qquad \psi_{s,K}(P) = -\frac{1}{2\pi} \iint_{\substack{\text{one side} \\ \text{of obstacle}}} \psi_{s,K} \frac{\partial}{\partial n}\left(\frac{e^{ik|\underset{\sim}{r} - \underset{\sim}{\rho}|}}{|\underset{\sim}{r} - \underset{\sim}{\rho}|}\right) dx\,dy$$

In particular, for our disk,

$$(11) \qquad \psi_{s,K}(P) = -\frac{1}{2\pi}\int_0^a\int_0^{2\pi} \frac{\partial}{\partial z}\left(\frac{e^{ik|\underset{\sim}{r} - \underset{\sim}{\rho}|}}{|\underset{\sim}{r} - \underset{\sim}{\rho}|}\right)\rho\,d\rho\,d\phi$$

Now,

$$(12) \qquad \begin{aligned} \frac{\partial}{\partial z}\left(\frac{e^{ik|\underset{\sim}{r} - \underset{\sim}{\rho}|}}{|\underset{\sim}{r} - \underset{\sim}{\rho}|}\right) &= \frac{\partial}{\partial z}\left[\frac{e^{ik\sqrt{r^2+\rho^2 - 2r\rho\cos(\frac{\pi}{2} - \theta)}}}{\sqrt{r^2+\rho^2 - 2r\rho\cos(\frac{\pi}{2} - \theta)}}\right] \\ &= \frac{\partial}{\partial z}\left[\frac{e^{ikr}}{r}\,e^{-ik\rho\sin\theta}\right], \\ &= ik\cos\theta\,\frac{e^{ikr}}{r}\,e^{-ik\rho\sin\theta} \end{aligned}$$

when $r \to \infty$, i.e. when $r \gg \rho$.

Thus, for large r,

$$\psi_{s,K} = - \frac{ik \cos\theta}{2\pi} \frac{e^{ikr}}{r} \int_0^a \int_0^{2\pi} e^{ik\rho \sin\theta} \rho \, d\rho \, d\phi ,$$

$$= - \frac{i \cos\theta}{k \sin^2\theta} \frac{e^{ikr}}{r} \int_0^{ka \sin\theta} J_0(x) x \, dx \quad ,^{*}$$

$$= - ia \frac{e^{ikr}}{r} \frac{J_1(ka \sin\theta)}{\tan\theta} \quad .^{**}$$

The flux of radiated power, R, on a surface completely enclosing the scatterer is in acoustics given by

$$(14) \qquad R = \frac{1}{2} \rho_0 ck \, \mathcal{R}e \left\{ i \, \psi_s \frac{\partial}{\partial n} \psi_s^{*} \right\} , \qquad 24.$$

the star denoting a complex conjugate, ρ_0 the equilibrium density, and c the phase velocity of sound in the medium. Consequently we obtain for the disk

$$(15) \quad \frac{r^2}{\rho_0 c} R_K \equiv \mathcal{R}_K(ka;\theta) = \frac{k^2 a^2}{2} \frac{J_1^{\,2}(ka \sin\theta)}{\tan^2\theta}$$

Graphs of $\mathcal{R}_K(ka;\ \theta)$, i.e. the radiation patterns, have been plotted against θ at the integer values of ka in $1 \leq ka \leq 5$. They are drawn in broken lines on figures 3 to 7.

3. Notes on Rigid Scatterers Lying in one Plane

We show here that one Kirchhoff condition, i.e. $\psi_s = 0$ on the plane of, but off the disk, is exact and not approximative as might easily be supposed.

Our proof is general in that it applies to all scatterers entirely confined to a plane***

---

* see Jahnke-Emde, Tables of Functions, (Dover Reprints, 1945) p. 149.

**see ibid., p. 145, article 6.

***For details of the proof the author is indebted to Dr. Eugene Isaacson of New York University.

The total field ψ is written

(16) $$\psi = \psi_{inc} + \psi_s ,$$

and each part of ψ satisfies the scalar wave equation (2). The function ψ_{inc} is a solution for free space, as if the scatterer were absent. It is continuous and bounded everywhere, except at the sources where it has singularities of type $\frac{1}{R}$. The same holds for its first and second derivatives. In the case of a plane incident wave, the source is removed to infinity. In no conventional diffraction problem is it assumed that the sources lie on the scatterer, and we will exclude that possibility from our observations here. The function ψ_s, its first and second derivatives are necessarily bounded and continuous in free space; at all points on the "infinite sphere" ψ_s and $\frac{\partial \psi_s}{\partial r}$ vanish for we require that conditions (7) be satisfied. At the scatterer, however,

(17) $$\frac{\partial \psi}{\partial n} = 0$$

and ψ_s and its first and second derivatives are not necessarily continuous. But the boundary condition allows us to make assertions on the properties of one of the derivatives of ψ_s. Using the xy plane for the plane of the scatterer as before, we find that $\frac{\partial \psi_s}{\partial z} = - \frac{\partial \psi_{inc}}{\partial z}$ on the positive side, $- \frac{\partial \psi_s}{\partial z} = \frac{\partial \psi_{inc}}{\partial z}$ on the negative side of the scatterer, because of (17), and therefore, since $\frac{\partial \psi_{inc}}{\partial z}$ is bounded and continuous across the scatterer, $\frac{\partial \psi_s}{\partial z}$ is also. Across the rest of the plane it is continuous. Let us denote a discontinuity by brackets $[\;]$.

(18) $$\left[\frac{\partial \psi_s}{\partial z}\right] = 0 \quad , \qquad z = 0 .$$

We proceed now to view the solution to problems based on the scalar wave equation (2) from the viewpoint of Green's functions. Within a closed surface S the value of ψ at P is given by an integral over S,

(19) $$\psi(P) = \int_S \left(\frac{\partial \psi}{\partial n} G - \psi \frac{\partial G}{\partial n}\right) dS ,$$

where G is a Green's function for the scalar wave equation so adjustable that it satisfies simple boundary conditions on S. Thus either G or $\frac{\partial G}{\partial n}$ may be made to vanish on S and consequently ψ is completely determined by either $\frac{\partial \psi}{\partial n}$ or ψ on S. We shall not give the details of this theory here.[25].

The Green's function for (2) in the infinite domain, for instance, is known to be $\frac{e^{ikR}}{4\pi R}$ where R is the distance from the variable point to P. When we consider, however, the semi-infinite domain obtained by dividing all space in two by an infinite plane, say z = 0, as in our case, then

$$(20) \qquad G = \frac{e^{ikR_1}}{4\pi R_1} \pm \frac{e^{ikR_2}}{4\pi R_2} \quad ;$$

the point P lies inside our semi-infinite domain; R_1 is the distance from P to the variable point Q' in our domain, see figure 2; R_2 is the distance from P to the mirror image of the variable point about the plane. The singularity of G arises from the one term only. Figure 2 illustrates this. The + sign is chosen if we wish that $\frac{\partial G}{\partial n} = 0$ on the plane; the minus sign for G = 0 on the plane, on which $R_1 = R_2$.

The surface S enclosing our domain is completed by the "infinite hemisphere". The functions ψ_s, G and $\frac{\partial \psi_s}{\partial n}$, $\frac{\partial G}{\partial n}$ vanish there. Consequently ψ_s is given in our problem by alternate integrals over the xy plane, e.g.

$$(21a) \qquad \psi_s(P) = \frac{1}{2\pi}\int_0^{2\pi}\int_0^{\infty} \frac{\partial \psi_s}{\partial n} \frac{e^{ikR}}{R} \rho \, d\rho \, d\phi$$

or

$$(21b) \qquad \psi_s(P) = -\frac{1}{2\pi}\int_0^{2\pi}\int_0^{\infty} \psi_s \frac{\partial}{\partial n} \frac{e^{ikR}}{R} \rho \, d\rho \, d\phi$$

for, when the variable point is confined to $z = 0$, $R_1 = R_2 = R$; and these integrals are taken over the values of ψ and $\frac{\partial \psi}{\partial n}$, respectively, on that side of $z = 0$ facing the semi-infinite domain under consideration, $z > 0$ or $z < 0$.

Since we know that $\frac{\partial \psi_s}{\partial z}$ is continuous across $z = 0$, relation (21a) proves that ψ_s is odd in z; for $\frac{\partial}{\partial n} = \pm \frac{\partial}{\partial z}$, respectively, on the two sides of $z = 0$.

When a function is odd in z, bounded, continuous across the origin, it is zero at the origin. Consequently

(22) $\psi_s = 0$ in the plane of the scatterer but off the scatterer.

A further conclusion may be drawn from the integral (21a), having to do with singularities in $\frac{\partial \psi_s}{\partial n}$ on the edge of the scatterer. We postpone discussion of this to Section 5

We have made no restrictions about the shape of the scatterer other than that it is plane. Our proof applies equally well to the infinite screen with one or more apertures of any shape.

This result is of significance in our discussion of the Kirchhoff theory of acoustic diffraction by the disk. We find that the only error of the theory lies in its assumptions for ψ_s on the surface of the disk.

Now, a relatively small error in the value of ψ_s on the surface of the disk should not be too significant at sufficiently large distance. One would think so, intuitively. Consequently we should not be too surprised if the Kirchhoff theory proves to be a powerful approximation method, applicable in a wide range of ka values, even when λ is not small when compared to the dimensions of the acatterer.

Another significant conclusion derives from this argument. We know now that no scatterers of the type under discussion produce a diffraction effect in their planes. For different scatterers of that type and of finite dimension, the values of ψ_s on the surface should of course be different. But the differences of ψ_s there are not great between, say, a circular or a square disk. Even if they are, their distant fields should be very similar, as a consequence, if we go sufficiently far away.

It should be mentioned here that our observations in the preceding two paragraphs hold equally well for diffraction by the infinite plane screen with an arbitrary aperture. This may not be immediately obvious because the "obstacle" per se is infinite. Nonetheless, our assertions hold, because the Kirchhoff conditions on ψ on the surface of the screen may be transformed into conditions on $\frac{\partial \psi}{\partial n}$ in the aperture - a theorem which we will not prove here.

Similar arguments may be applied to electromagnetic diffraction by a perfect conductor confined to a plane. We would find that the tangential electric vector must be even, the tangential magnetic vector odd, across the plane.

It is hoped that the foregoing general discussion yields some insight into certain problems of diffraction. As regards the problem for the disk in particular, we have already obtained approximation values for the acoustic radiation pattern of a disk in a wide range of ka, cf. equation (15) and figures 3 to 7.

The only assumption we made to obtain this was to say that ψ is 2 on the positive side and 0 on the negative side of a rigid disk illuminated by a normally incident plane wave of unit amplitude. It is now of interest to know the exact value, in order to compare with these

assumptions. Two ways of achieving this are open to us. One is to use Wiener's experimental data taken with a specially constructed pressure microphone[22]. The other is to evaluate the appropriate quantities from the exact spheroidal theory of Bouwkamp[15] and Spence[14].

We proceed therefore to consider the exact field scattered by the rigid circular disk, in particular, (i) on its surface, and (ii) the radiation pattern at large distances. The latter will serve to appraise the results of the Kirchhoff radiation theory.

4. Summary of the Wave Functions of the Oblate Spheroid of Order Zero.

It is necessary to recapitulate here in brief the analysis of the wave functions of this problem. As such this section reviews or makes use of the work of a number of authors, but the details of all matters summarized here may be found in the paper by Spence[14].

When considering normal incidence the entire field is independent of ϕ. When the wave equation (2) is separated, the ϕ dependence is identical to that in all other systems with coordinate surfaces which are surfaces of revolution, i.e., a ϕ dependence $e^{\pm im\phi}$ see equation (5). Here, then, m = 0, and this restricts us to the so-called functions of order zero.

The spheroidal coordinates are related to the cartesian coordinates by the set of equations

$$(23)\qquad \begin{aligned} x &= a(1+\xi^2)^{1/2}(1-\eta^2)^{1/2}\cos\phi , \\ y &= a(1+\xi^2)^{1/2}(1-\eta^2)^{1/2}\sin\phi , \\ z &= a\xi\eta ; \end{aligned}$$

the metric coefficients of the system are then easily found from the equality $dx^2 + dy^2 + dz^2 = h_\eta^2\, d\eta^2 + h_\xi^2\, d\xi^2 + h_\phi^2\, d\phi^2$:

$$(24)\qquad h_\eta = a\left(\frac{\xi^2+\eta^2}{1-\eta^2}\right)^{1/2}, \quad h_\xi = a\left(\frac{\xi^2+\eta^2}{1+\xi^2}\right)^{1/2},$$

$$h_\phi = a(1-\eta^2)^{1/2}(1+\xi^2)^{1/2} .$$

The differential equations for the angular and radial wave-functions of the oblate spheroid and of order zero are

$$(25)\quad (1-\eta^2)\frac{d^2 u_\ell}{d\eta^2} - 2\frac{d u_\ell}{d\eta} + (\alpha_\ell - k^2a^2(1-\eta^2))\,u_\ell = 0,$$

$$(26)\quad (1+\xi^2)\frac{d^2 v_\ell}{d\xi^2} + 2\xi\frac{d v_\ell}{d\xi} - (\alpha_\ell - k^2a^2(1+\xi^2))\,v_\ell = 0,$$

respectively, and are obtained by separating (2) in our system according to $\psi_\ell = u_\ell(\eta)\, v_\ell(\xi)$. We are using a notation adapted from the work of Page on the prolate spheroid[26]. The index ℓ takes on integer values from zero to infinity and refers to eigenfunctions, i.e. solutions at prescribed values, or eigenvalues, of the separation constant α, namely α_ℓ. They arise as follows: The angular equation has regular singular points at $\eta = \pm 1$, with double indicial roots equal to zero at both values. When $\eta = \pm 1$ we refer to points on the z axis which are points included in the physical problem. The so-called solutions of the first kind are analytic at the regular singular points at and only at special values of α.

Thus - again following Page in our analysis of the functions, near the origin of the arguments - let us expand the first solutions about the singular points of (25). It is then found that these are either even or odd in η. One obtains

$$(27)\qquad u_\ell = \sum_{k=0}^{\infty} c^{\ell}_{2k}(1-\eta^2)^k \qquad ,\ \ell \text{ even},$$

or

$$(28)\qquad u_\ell = \eta\sum_{k=0}^{\infty} c^{\ell}_{2k}(1-\eta^2)^k \qquad ,\ \ell \text{ odd},$$

and these series converge everywhere in $-1 \leq \eta \leq 1$, if and only if, the separation constant takes on values

$$(29)\qquad \alpha_\ell = \ell(\ell+1) + \gamma_\ell(k^2a^2)$$

where $\gamma_\ell(k^2a^2)$ are prescribed functions of k^2a^2 and different for different ℓ. The index ℓ and the values of α_ℓ arise naturally from an analysis of the convergence properties, which one may study from the recursion formulas for the c^ℓ_{2K}. It is not possible to give all details here. The reader should refer to the paper by Spence. All $\gamma_\ell(o) = 0$, and (25) becomes Legendre's equation when ka = 0. Hence the u_ℓ may be so normalized that

(30) $$u_\ell\,(\eta,\ ka = 0) = P_\ell\,(\eta),$$

the Legendre polynomials. This normalization is obtained by letting the c^ℓ_o be equal to unity. The functions are orthogonal, and their norms

(31) $$N_\ell = \int_{-1}^{+1} u^2_\ell\,(\eta)\,d\,\eta$$

may be easily computed at the different values of ka.

When the two indicial roots, at a regular singular point of a second order differential equation, are repeated and zero, the solution "of the second kind" necessarily possesses a logarithmic singularity at that point. This solution is ruled out from our angular functions, for the singular points are included in our physical space.

But this does not apply to the radial functions which satisfy (26). We note that the radial functions are obtained from the angular function by letting η assume imaginary values. The singular points are at $\xi = \pm$ i, not a part of physical space.

Thus we have to consider radial functions of both kinds. Those of the first kind are simply chosen as

(32) $${}^{(1)}v_\ell\,(\xi) = \frac{1}{(1,i)\sum c^\ell_{2K}}\,u_\ell\,(i\,\xi)\,.$$

The factor 1 in (1,i) is to be used when ℓ is even, the factor i when it is odd; it ensures that the ${}^{(1)}v_\ell\,(\xi)$ are all real at real ξ. The functions are normalized such that they have convenient values on the disk, i.e.

(33) $${}^{(1)}v_\ell(0) = 1, \text{ when } \ell \text{ even},$$

(34) $${}^{(1)}v_\ell{}'(0) = 1, \text{ when } \ell \text{ odd},$$

where a prime denotes the derivative.

The functions of the second kind can be shown to have the form

$$(35) \qquad {}^{(2)}v_\ell(\xi) = Q_\ell \left\{ {}^{(1)}v_\ell(\xi)\,(\tan^{-1}\xi - \tfrac{\pi}{2}) + g_\ell(\xi) \right\}$$

where $g_\ell(\xi)$ is odd when ℓ is even and even when ℓ is odd, and is known to be analytic at the singular points $\xi = \pm i$. At these points $\tan^{-1}\xi$ has logarithmic singularities. The Q_ℓ are as yet arbitrary normalization coefficients.

As Poole has first shown[27], the radial functions can be expressed by integrals containing the angular functions $u_\ell(\eta)$. These may be used to good advantage in evaluating the $v_\ell(\xi)$ at large arguments where the spheroids are nearly spheres,

$$(36) \qquad r \sim a\xi \,, \quad \xi \gg 0.$$

Thus, it may be proven that

$$(37) \qquad {}^{(1)}v_\ell(\xi) = \frac{q_\ell}{2}\int_{-1}^{1} e^{ika\xi\eta}\, u_\ell(\eta)\, d\eta \,.$$

The coefficients q_ℓ depend on normalization and we already have, by means of (33) and (34), fixed the normalization of the ${}^{(1)}v_\ell(\xi)$. Consequently the q_ℓ are completely determined functions of ka and may be computed numerically. What is more important, however, a radial function ${}^{(3)}v_\ell(\xi)$ may be defined by the integral

$$(38) \qquad {}^{(3)}v_\ell(\xi) = q_\ell \int_{i\infty}^{1} e^{ika\xi\eta}\, u_\ell(\eta)\, d\eta \,,$$

which one may show to be

$$(39) \qquad {}^{(3)}v_\ell(\xi) = {}^{(1)}v_\ell(\xi) + i\,{}^{(2)}v_\ell(\xi) \,,$$

and which has the further property that

$$(40) \qquad {}^{(3)}v_\ell(\xi) \sim \frac{e^{ika\xi}}{ka\xi} = \frac{e^{ikr}}{kr} \,, \quad \xi \to \infty$$

That is to say, eigenfunctions Ψ_ℓ, containing ${}^{(3)}v_\ell$ as their radial part, satisfy Sommerfeld's conditions (6) and therefore behave as radially diverging waves. The scattered field Ψ_s must be made up of these eigenfunctions.

Since the q_ℓ are already known in (38), the values of the Q_ℓ in (35) may be determined, and numerically tabulated for the different values of ℓ and ka. We now have indicated the procedures necessary to obtain all the quantities needed in a solution of the acoustic disk problem (at normal incidence).

The functions $\psi_\ell(\xi, \eta)$ discussed above form a complete orthogonal set. It is possible therefore to expand other functions of the same variables in terms of the ψ.

Thus we may write

$$(41) \qquad e^{-ikz} = \sum_{\ell=0}^{\infty} A_\ell \, u_\ell(\eta) \, v_\ell(\xi)$$

for the plane wave incident normal to the disk; in this series both the A_ℓ and the kind of funtion $v_\ell(\xi)$ are unknown but - using (31),(23) and (37),

$$(42) \qquad A_\ell N_\ell v_\ell(\xi) = \int_{-1}^{1} e^{-ikz} u_\ell(\eta)\, d\eta$$

$$= \int_{-1}^{1} e^{-ika\xi\eta} \, u_\ell(\eta)\, d\eta$$

$$= (-)^\ell \frac{2}{q_\ell} \, {}^{(1)}v_\ell(\xi).$$

Consequently the radial functions in (41) are of the first kind and

$$(43) \qquad A_\ell = \frac{2(-)^\ell}{N_\ell q_\ell}.$$

The total velocity potential in the disk-problem may be similarly expanded:

$$(44) \quad \psi = \psi_{inc} + \psi_s$$

$$= \sum_{\ell=0}^{\infty} \frac{2(-)^\ell}{N_\ell q_\ell} u_\ell(\eta)\, {}^{(1)}v_\ell(\xi) + \sum_{=0}^{\infty} B_\ell u_\ell(\eta)\, {}^{(3)}v_\ell(\xi),$$

where the B_ℓ are coefficients to be determined by the acoustic boundary condition at the disk, namely

(45) $$\frac{\partial \Psi}{\partial \xi} = 0 \quad \text{at} \quad \xi = 0.$$

Thus, one obtains

(46) $$B_\ell = \frac{2}{N_\ell \, q_\ell \, {}^{(3)}v_\ell'(0)}, \quad \ell \text{ odd}$$

$$B_\ell = 0, \ \ell \text{ even},$$

as found in Spence's paper. We note that Ψ_s has become odd in η as a direct consequence of applying condition (45).

5. The Exact Values of the Near and Distant Fields.

Small fluctuations in a compressible fluid are governed by the relation

(47) $$\underset{\sim}{v} = -\nabla \Psi$$

where $\underset{\sim}{v}$ is the velocity vector, irrotational, since its curl vanishes, and by the equation of motion,

(48) $$\frac{\partial \underset{\sim}{v}}{\partial t} + \frac{1}{\rho_0} \nabla p = 0,$$

where p is the pressure. Consequently the essential physical quantities are given in terms of the velocity potential, and, in the case of monochromatic acoustical oscillations with harmonic time dependence $e^{-i\omega t}$, the pressure is simply proportional to Ψ,

(49) $$p = -i\omega\rho_0 \Psi .$$

Thus the entire diffracted field may be investigated by means of the expressions

(50) $$\Psi_s = \sum_{\ell \text{ odd}} \frac{2}{N_\ell \, q_\ell \, {}^{(3)}v_\ell'(0)} \, u_\ell(\eta) \, {}^{(3)}v_\ell(\xi),$$

$$(51) \quad \nabla \psi_s = \left(\frac{\underset{\sim}{\eta}_1}{h_\eta} \frac{\partial}{\partial \eta} + \frac{\underset{\sim}{\xi}_1}{h_\xi} \frac{\partial}{\partial \xi} \right) \psi_s$$

$$= \sum_{\ell \text{ odd}} \frac{2}{aN_\ell q_\ell} \left\{ \underset{\sim}{\eta}_1 \left(\frac{1-\eta^2}{\xi^2+\eta^2} \right)^{1/2} u_\ell'(\eta) \frac{{}^{(3)}v_\ell(\xi)}{{}^{(3)}v_\ell'(0)} + \right.$$

$$\left. + \underset{\sim}{\xi}_1 \left(\frac{1+\xi^2}{\xi^2+\eta^2} \right)^{1/2} u_\ell(\eta) \frac{{}^{(3)}v_\ell(\xi)}{{}^{(3)}v_\ell'(0)} \right\} .$$

Here $\underset{\sim}{\eta}_1, \underset{\sim}{\xi}_1$, are unit vectors orthogonal to the hyperbolas and ellipses of figure 1, respectively.

A. Singularities at the Edge

Singularities at the edge of the disk occur only in certain velocity components, not in pressure, and are mathematically a direct consequence of the presence of the metric coefficients in the expression for gradient.

On the surface of the disk $\xi = 0$, and we obtain

$$(52) \quad \underset{\sim}{v}_s(0,\eta) = - \sum_{\ell \text{ odd}} \frac{2}{N_\ell q_\ell} \left\{ \underset{\sim}{\eta}_1 \frac{{}^{(3)}v_\ell(0)}{{}^{(3)}v_\ell'(0)} (1-\eta^2)^{1/2} \frac{u_\ell'(\eta)}{a\eta} + \right.$$

$$\left. + \underset{\sim}{\xi}_1 \frac{u_\ell(\eta)}{a\eta} \right.$$

The tangential velocity component vanishes at the center of the disk, $\eta = \pm 1$, while the normal component

$$(53) \quad |\underset{\sim}{v}|_{s,\xi}(0,\eta) = - \sum_{\ell \text{ odd}} \frac{2}{aN_\ell q_\ell} \frac{u_\ell(\eta)}{\eta} = \left\{ \left[\frac{\partial}{a\eta\partial\xi} \right] \sum_{\ell=0}^{\infty} \frac{2(-)^\ell}{N_\ell q_\ell} u_\ell(\eta) {}^{(1)}v_\ell(\xi) \right\}_{\xi=0}$$

for $v_\ell'(o) = 0$, when ℓ is even, $v_\ell'(o) = 1$ when ℓ is odd. On the surface of the disk, one may easily show that

$$(54) \quad \left(\frac{\partial}{\partial z} \right)_{\xi=0} = \left(\frac{\partial \eta}{\partial z} \frac{\partial}{\partial \eta} + \frac{\partial \xi}{\partial z} \frac{\partial}{\partial \xi} \right)_{\xi=0} = \frac{\partial}{a\eta\partial\xi}$$

Therefore, using (41) and (43)

$$(55) \quad |\underset{\sim}{v}|_{s,\xi}(0,\eta) = \left(\frac{\partial}{\partial z} e^{-ikz} \right)_{\xi=0} = -ik,$$

a constant over the entire disk and equal and opposite to the normal velocity due to the incident field,

$$(56) \qquad -\left(\frac{\partial \Psi_{inc}}{\partial n}\right)_{z=0} = -\frac{\partial}{\partial z} e^{-ikz} = ik.$$

As we near the edge of the disk from its central portion, i.e. $\xi = 0$, $\eta \to 0$, the tangential velocity component varies as:

$$\frac{1}{\eta},$$

for, in (52) $|\underset{\sim}{v}|_{s,\eta}(0,\eta)$ varies as the $\frac{u_\ell'(\eta)}{\eta}$, ℓ odd, which have just such a singularity, since the derivatives of the odd functions are even and therefore non-zero at $\eta = 0$. Let ρ denote the radius vector from the center to any point on the disk,

$$(57) \qquad \rho = \left[(x^2+y^2)^{1/2}\right]_{\xi=0} = a(1-\eta^2)^{1/2}$$

and so

$$(58) \qquad \frac{1}{a\eta} = \frac{1}{(a^2-\rho^2)^{1/2}} \sim \frac{1}{(a-\rho)^{1/2}} \quad \text{as } \rho \to a$$

that is, $|\underset{\sim}{v}|_{s,\eta}(0,\eta)$ possesses a singularity of degree $\frac{1}{2}$, as a function of distance from the edge.

Thus we see that singularities of a certain type arise, as might be expected, but only in the free component - that on which no boundary condition is imposed; and that the "radial" velocity varies most rapidly near the edge.

On the remainder of the plane of the disk $\eta = 0$, and it is clear from (52) that the ξ component vanishes on this surface. This is the tangential component here, and the result is obvious, considering that Ψ_s vanishes by virtue of (22).

$$(59) \qquad \underset{\sim}{v}_s(\xi,0) = \underset{\sim}{\eta} \sum \frac{2u_\ell'(0)}{aN_\ell\, q_\ell\, {}^{(3)}v_\ell'(0)} \; \frac{{}^{(3)}v_\ell(\xi)}{\xi} \qquad .$$

As we approach the edge of the disk, $|\underset{\sim}{v}|_{s,\eta}(\xi, 0)$ has a singularity of the type:

$$\frac{1}{\xi},$$

for the functions ${}^{(3)}v_\ell(\xi)$, ℓ odd, contain the even part $iQ_\ell g_\ell(\xi)$, non-zero at the disk, which follows from (39) and (35). This is equivalent to a singularity of the type:

$$\frac{1}{(\rho - a)^{1/2}},$$

where ρ is the radius vector from the origin of our system to any point on $\eta = 0$, and hence $(\rho - a)^{1/2}$ measures distance to the edge. For now

$$(60) \qquad \rho = \left[(x^2 + y^2)^{1/2}\right]_{\eta = 0} = a(1 + \xi^2)^{1/2},$$

and

$$(61) \qquad (\rho^2 - a^2)^{1/2} = (\rho - a)^{1/2}(\rho + a)^{1/2} = a\xi .$$

It is clear that in all real scatterers the tangential flow is smooth on the surface, since in those cases we deal with smooth surfaces. The singularity arises as a limit in idealized cases in which infinite curvature may occur on the surface.

A general theorem about singularities at the edge of obstacles confined to a plane may be derived from the integral (21a). Returning, therefore, to the discussion in Section 3, let us consider field points P at the edge, We place the origin of coordinates into the point on the edge, for convenience. Then $R = \rho_Q$, where Q is the variable point.

The first integral becomes

$$(62) \qquad \Psi_s(P) = \frac{1}{2\pi}\int_0^{2\pi}\int_0^{\infty} \frac{\partial \Psi_s(Q)}{\partial n} e^{ik\rho_Q} \, d\rho_Q \, d\phi .$$

This integral diverges if and only if the behavior of $\dfrac{\partial \Psi_s}{\partial n}$ is such that

$\dfrac{\partial \Psi_s}{\partial n} \sim \dfrac{1}{\rho_Q^{\,p}}$, $p \geq 1$, at the edge, and will converge for $p < 1$. Consequently we have here the upper bound for singularities in the velocity components on z=0 near the edge.

B. The Pressure on the Disk.

Here we calculate the distribution of pressure over the disk by the exact theory. The results will serve for comparison with the Kirchhoff assumptions, i.e., that $\Psi = 2$ on the positive side, $\Psi = 0$ on the negative side, and for comparison with the experimental results of Wiener for the same quantity. Wiener measured the absolute value of total sound pressure in waves from a source sufficiently far from a thin metal disk to consider them as plane waves; the pressure was found at points on the disk's surface, and at the same points in the absence of the disk. The ratio $|p/p_{inc}|$ was then plotted against position on the surface. For normal incidence the data can be averaged over the azimuth φ, of which they are theoretically independent and are functions only of ρ, $0 \leq \rho \leq a$. In our solution

(63) $$(p_{inc})_{\xi=0} = -i\omega\rho_0 ,$$

by (49) and (41);

(64) $$\left| \frac{p}{p_{inc}} \right|_{\xi=0} = (|\psi|)_{\xi=0} = (|\psi_{inc} + \psi_s|)_{\xi=0}$$

$$= \left| 1 + \sum_{\ell \text{ odd}}^{\infty} \frac{2}{N_\ell \, q_\ell} \; \frac{{}^{(3)}v_\ell(0)}{{}^{(3)}v_\ell'(0)} \, u_\ell(\eta) \right| ,$$

which is in such a form that it may now be numerically computed from tables of the oblate spheroidal wave functions.

Our values are plotted in heavy lines on the schematic graphs of figures 8 to 12, separately for the ka = 1,2,3,4,5. For each ka the quantity $|p/p_{inc}|$ was found at ρ = 0, .341a, .6a, .8a, a, on both sides of the disk. The values on the positive or illuminated side of the disk are plotted upwards, on the negative or shadow side downwards. The experimental results are plotted on this graph in broken lines.

As ka increases the number of resonance peaks on the bright side increases, and, on the shadow side, a bright spot becomes increasingly pronounced. This latter phenomenon is not predicted by the Kirchhoff theory at all. However, since the distribution on the illuminated side

at ka = 5 differs little from the value 2, it would seem that the distribution is nearly that predicted by the theory at a ka as small as 5. But we should not draw the conclusion from this that the approximate assumptions on the near field, illuminated side, are good for all ka > 5 unless we had data for this region. In fact the experimental results at ka > 5 s show that this is not true. The reader is referred to additional curves plotted by Wiener[22] for further information.

Concerning agreement between theory and experiment - Wiener's experimental data are also plotted in figures 8 and 9 - it is, on the whole, good and lies within the expected error in the measurements, with some exceptions. The error is relatively large in such measurements, is greatest where the rate of change in pressure is largest and increases with frequency. There is also the inherent error due to diffraction by the microphone, and attached equipment near the disk. The exceptions are, (a) the discrepancy at $\rho=0$, ka=5, on the bright side, (b) the nearly constant difference across the disk at ka=2 and 3 on both sides; we know so far no reasons for this discrepancy. Furthermore we should not expect that the experimental values agree with ours at or near the edge of the disk on account of the fact that the real disk is of finite thickness.

Across the edge, the theoretical curves are continuous, while the slope is not. This fact is clear in view of our observations above on the singularities in the derivatives of ψ_s at the edge of the disk.

C. Radiation Patterns

When we substitute the equations (50) and (51), evaluated at large distance, in the formula (14) for the power flux, we obtain the exact value for $\mathcal{R}(ka;\theta)$:

$$(65) \qquad \mathcal{R}(ka;\theta) = 2 \sum_{\ell,}^{\infty} \sum_{\ell' \text{odd}}^{\infty} B_{\ell\ell'} u_{\ell}(\cos\theta)\, u_{\ell'}(\cos\theta) ,$$

for $\eta \rightarrow \cos\theta$ as $\xi \rightarrow \infty$; one finds that

$$(66) \qquad B_{\ell\ell'} = \frac{1 + (\pi^2 Q_\ell Q_{\ell'})/4}{N_\ell N_{\ell'} \left[1 + (\pi^2 Q^2)/4\right]\left[1 + (\pi^2 Q_{\ell'}^2)/4\right]} .$$

The quantity $\mathcal{R}(ka;\ \theta)$ was computed for ka = 1,2,3,4,5 at six different values of θ between 0 and $\pi/2$, and is shown graphically in the heavy lines of figures 3 to 7.

At ka = 1, where $\lambda = 2\pi a$, a large difference exists between $\mathcal{R}$ and $\mathcal{R}_K$. As ka increases the curves oscillate about each other with obviously decreasing amplitude; at ka = 5, where $\lambda = 1.25a$ the two curves very closely agree and it may be inferred safely that when ka > 5 the discrepancies between $\mathcal{R}$ and $\mathcal{R}_K$ will remain small. Hence we find that the Kirchhoff theory, allegedly applicable only as ka $\rightarrow \infty$, gives good approximate results at intermediate values of this quantity, also.

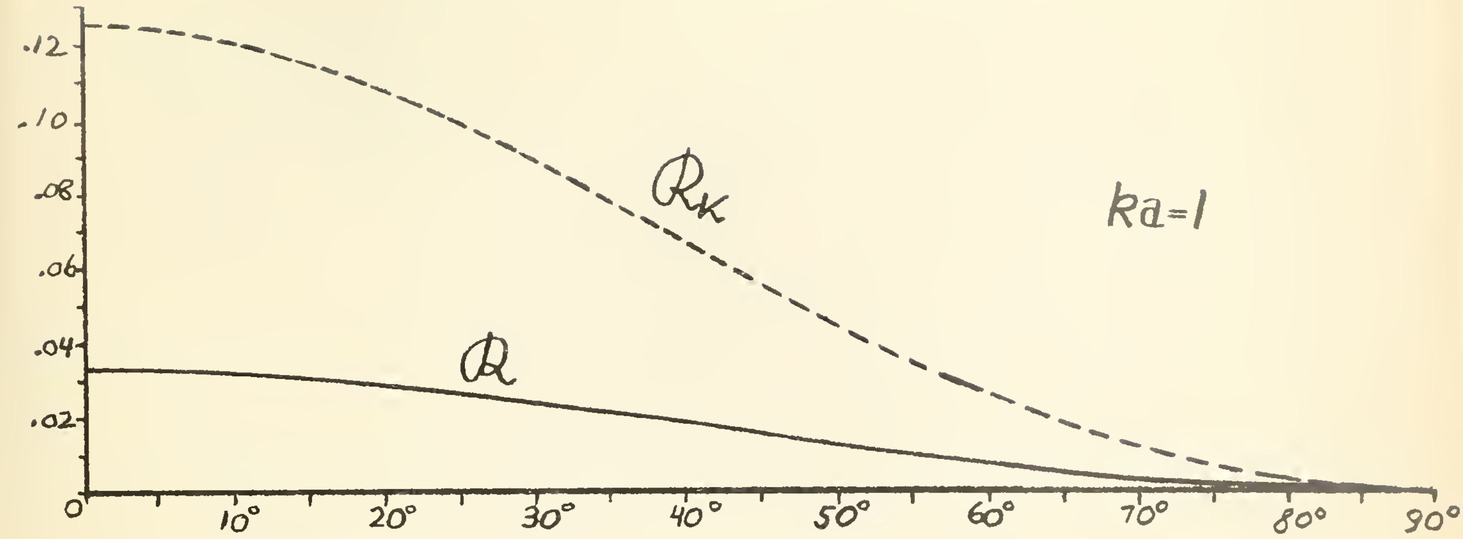

Figure 3

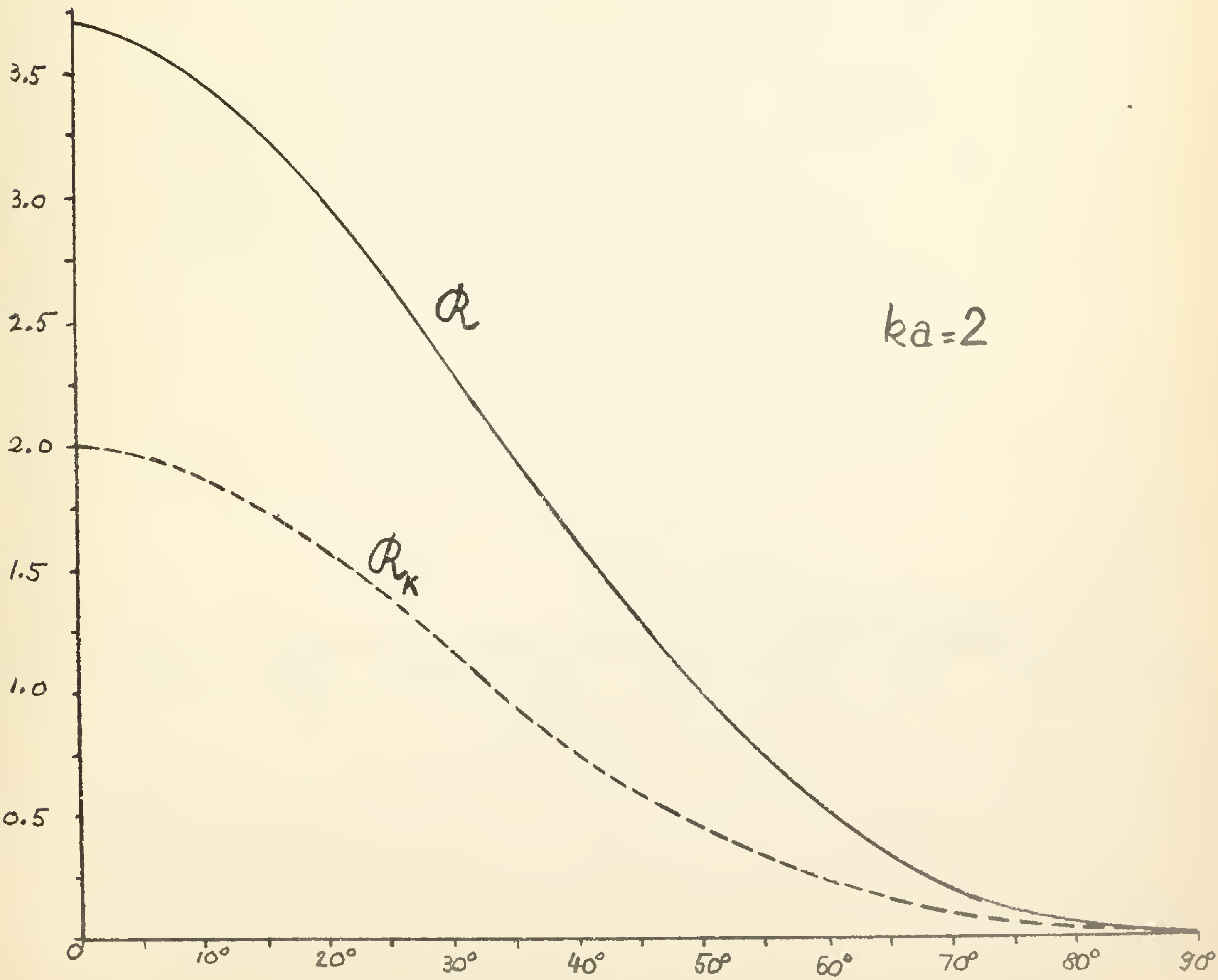

Figure 4

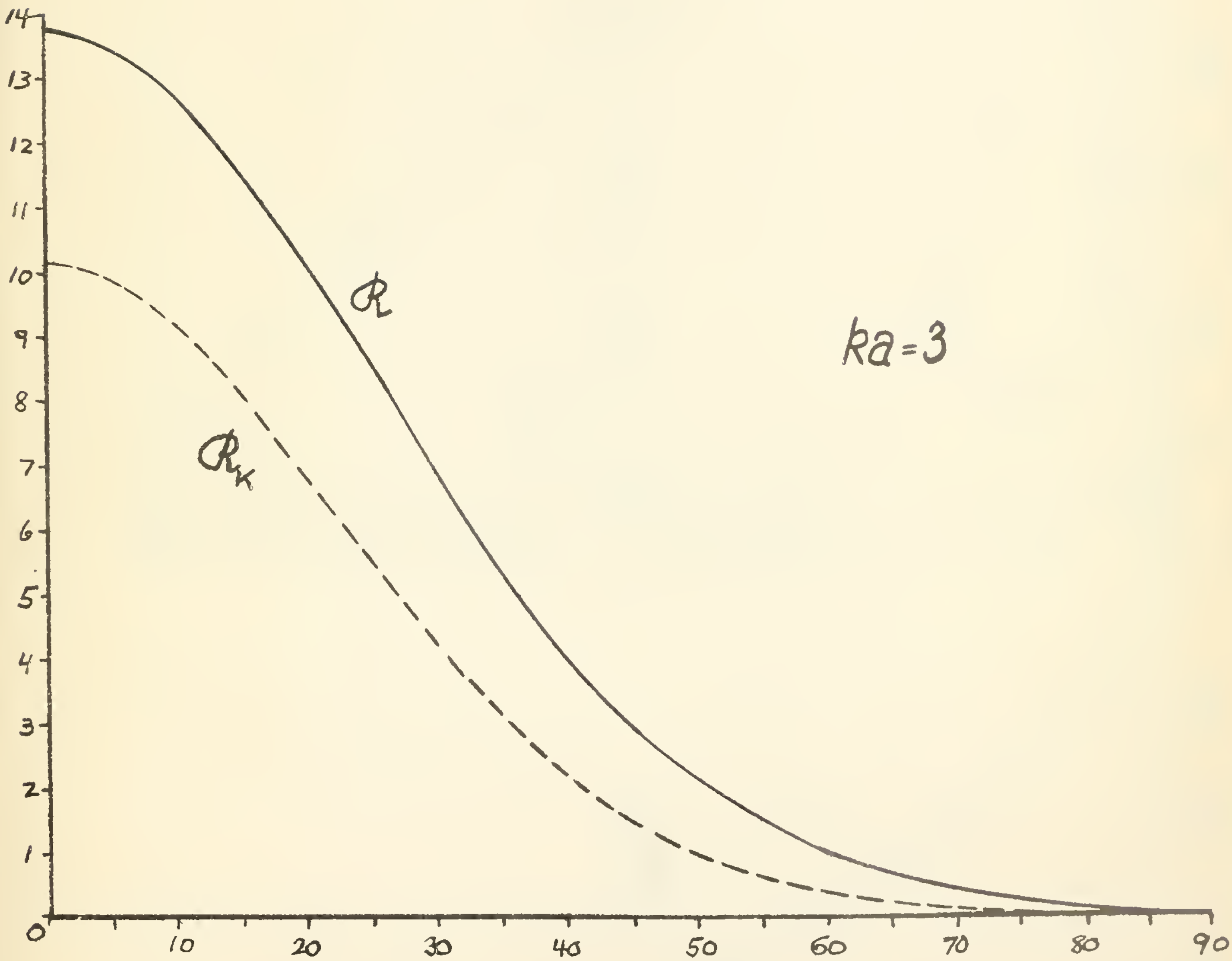
14
13
12
11
10
9
8
7
6
5
4
3
2
1
0
10
20
30
40
50
60
70
80
90
$\mathcal{R}$
$\mathcal{R}_K$
ka=3

Figure 5

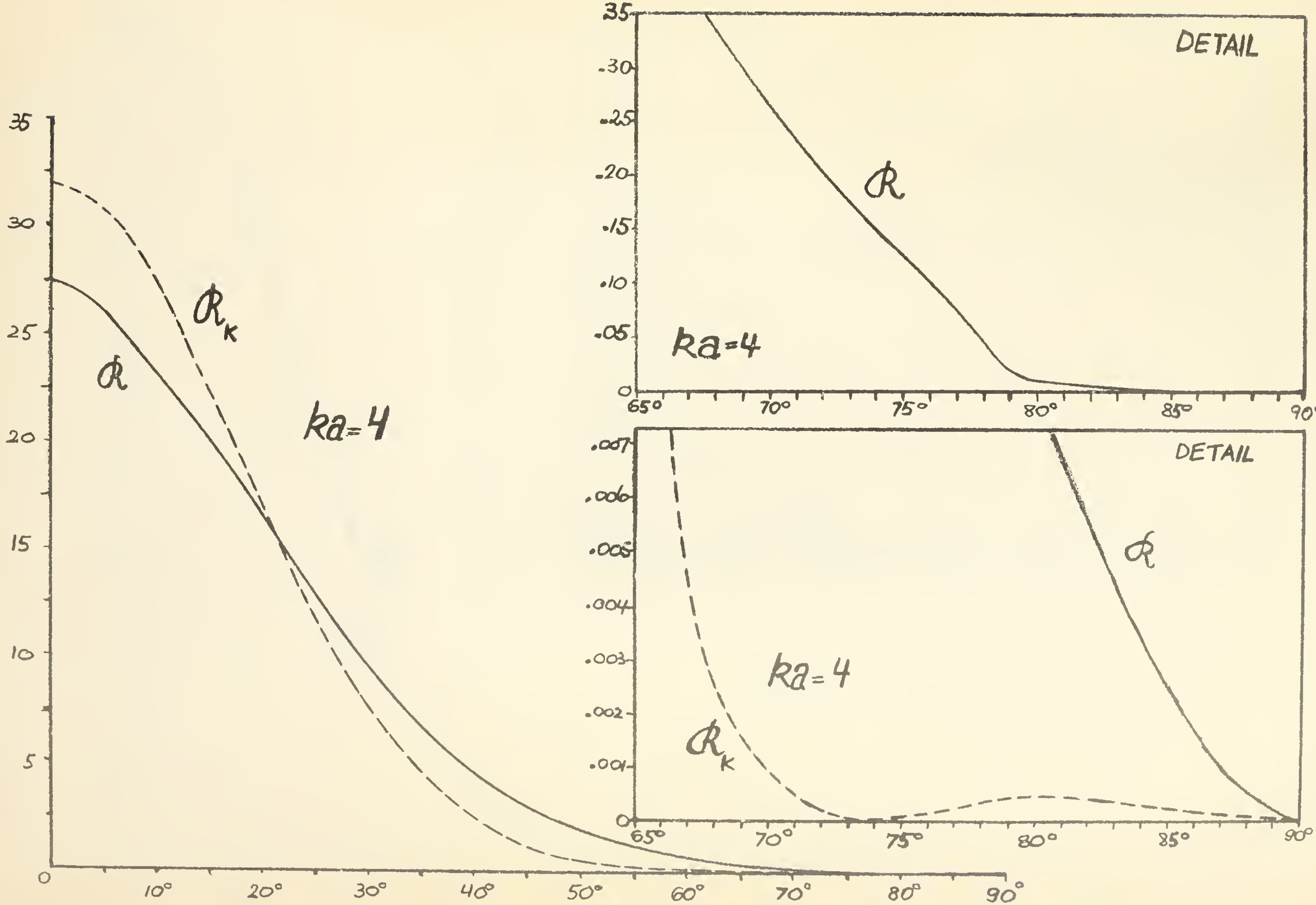

35
30
25
20
15
10
5
0
10°
20°
30°
40°
50°
60°
70°
80°
90°
$\mathcal{R}_k$
$\mathcal{R}$
ka=4
DETAIL
.35
.30
.25
.20
.15
.10
.05
65°
70°
75°
80°
85°
90°
.007
.006
.005
.004
.003
.002
.001

Figure 6

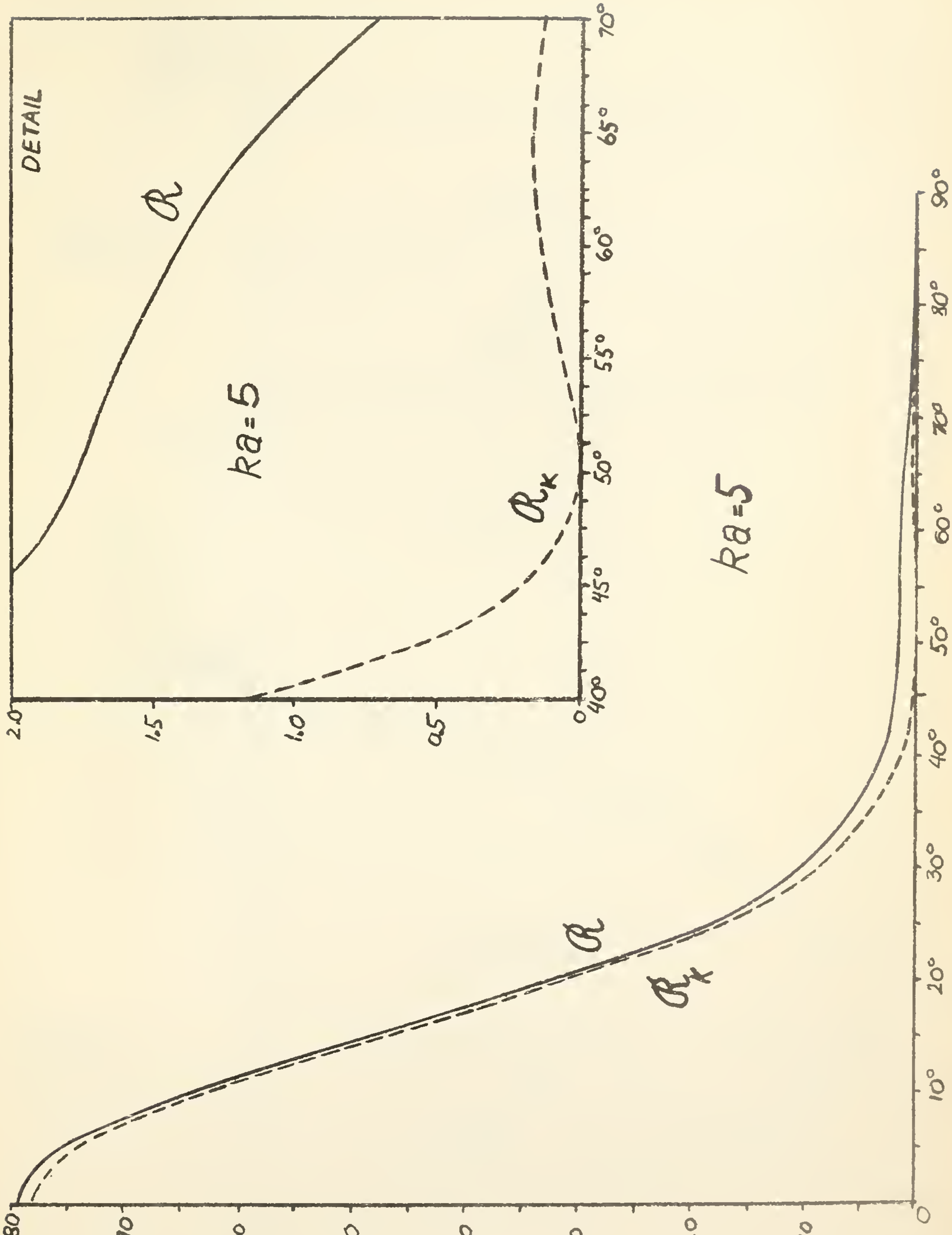
DETAIL
ka=5
ka=5
2.0
1.5
1.0
0.5
0
40°
45°
50°
55°
60°
65°
70°
80
70
60
50
40
30
20
10
0
10°
20°
30°
40°
50°
60°
70°
80°
90°

Figure 7

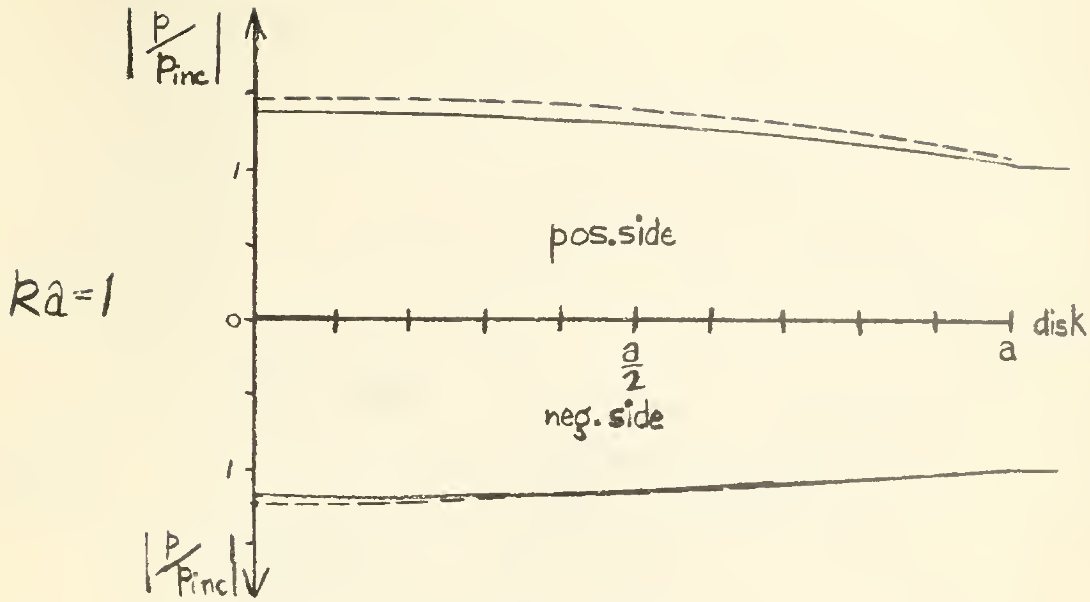

Figure 8

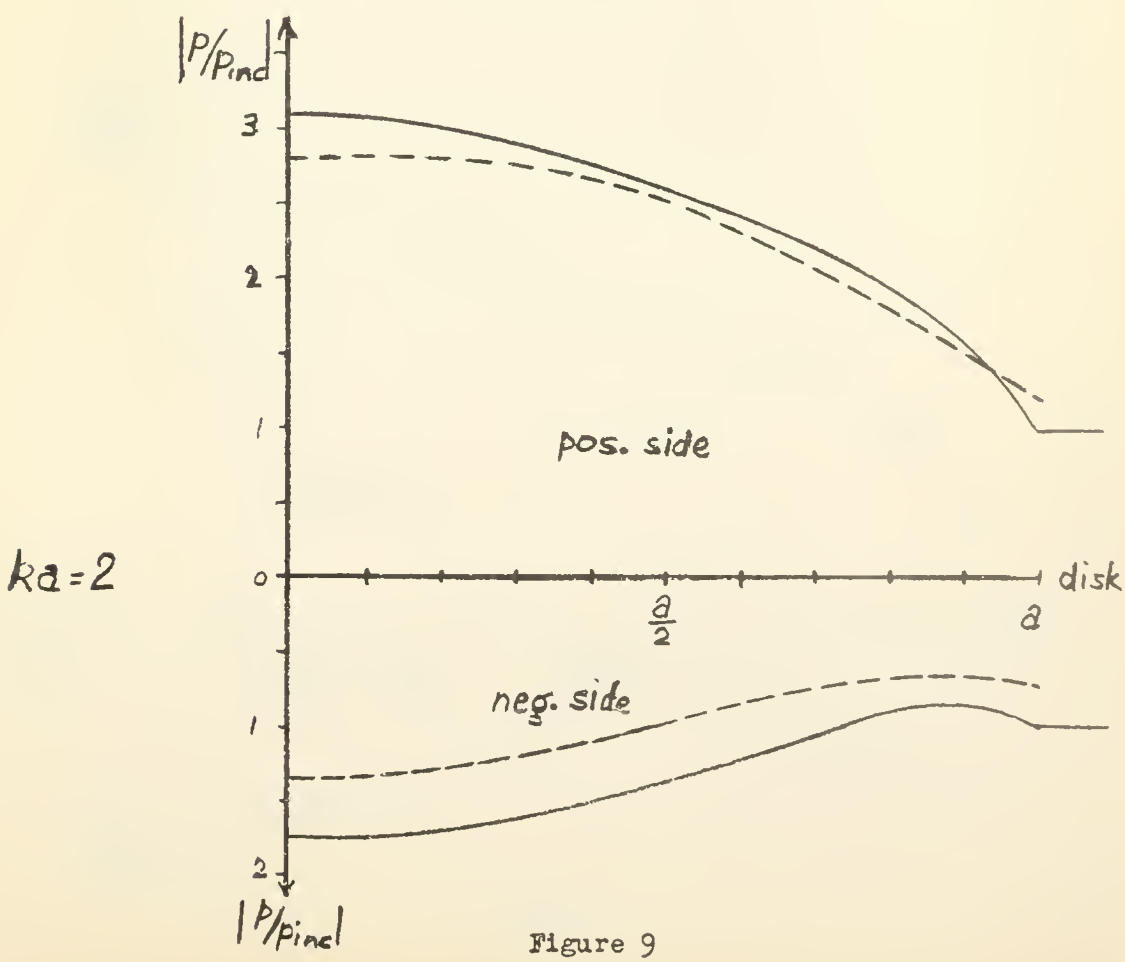

Figure 9

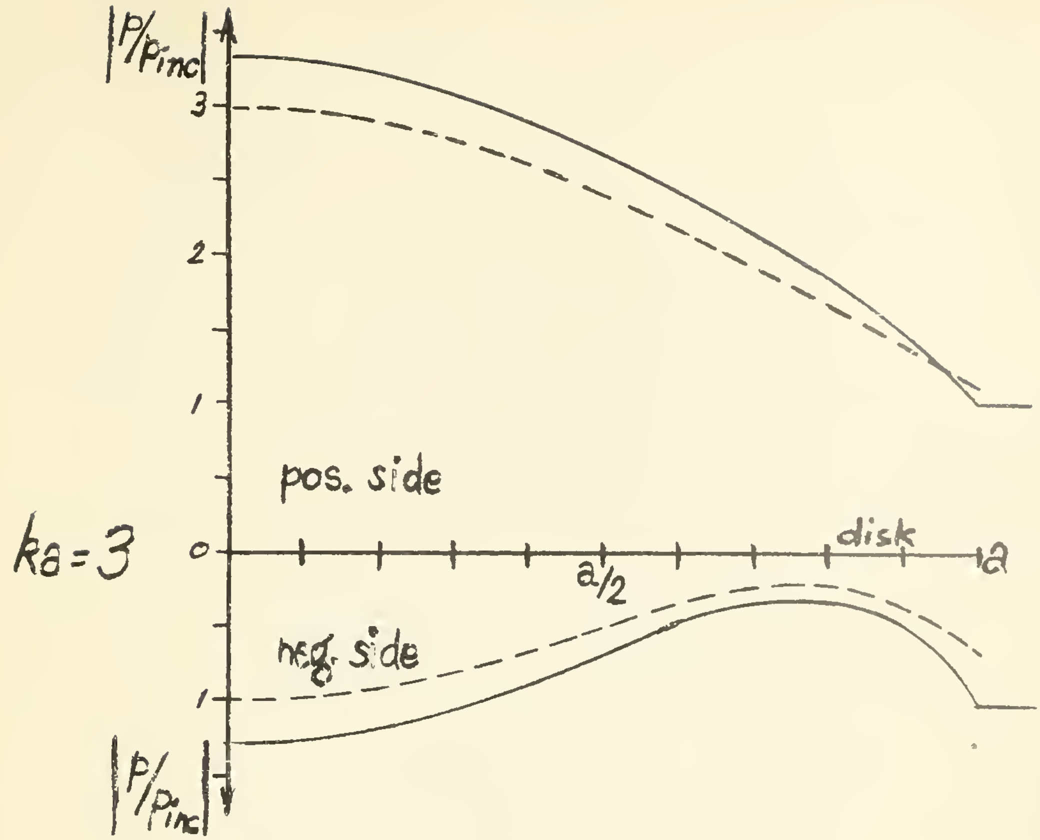

Figure 10

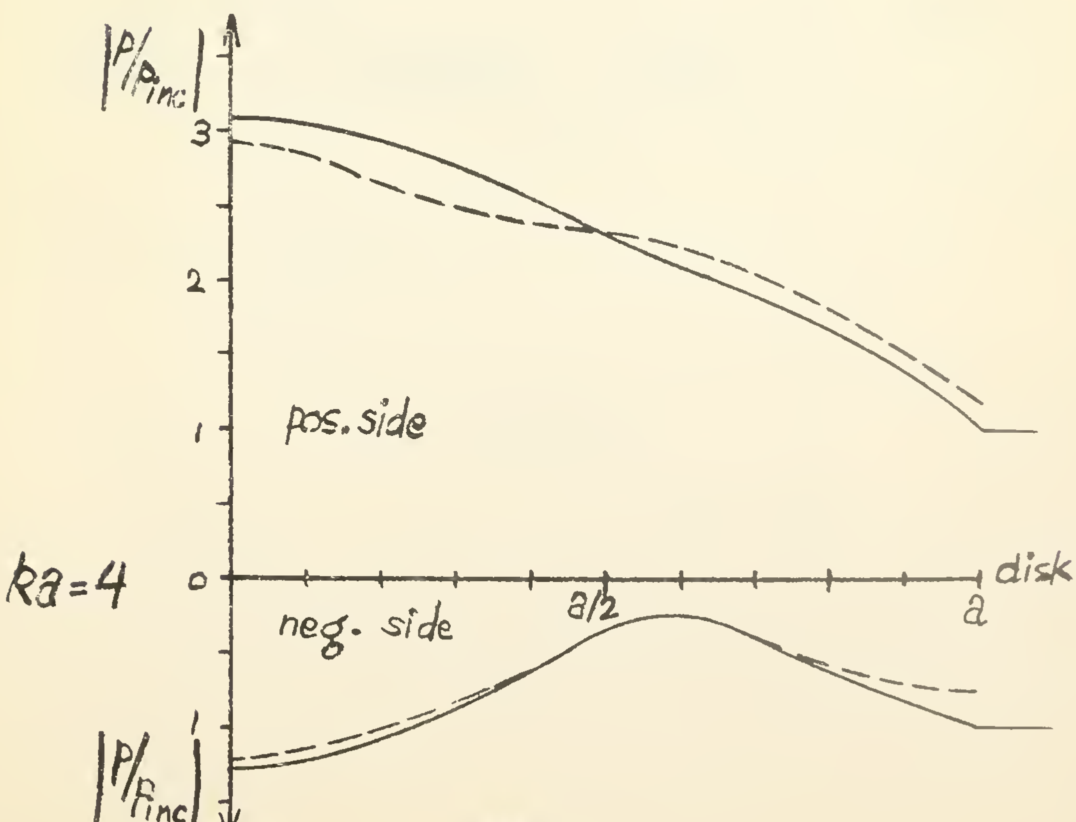

Figure 11

$ka = 5$

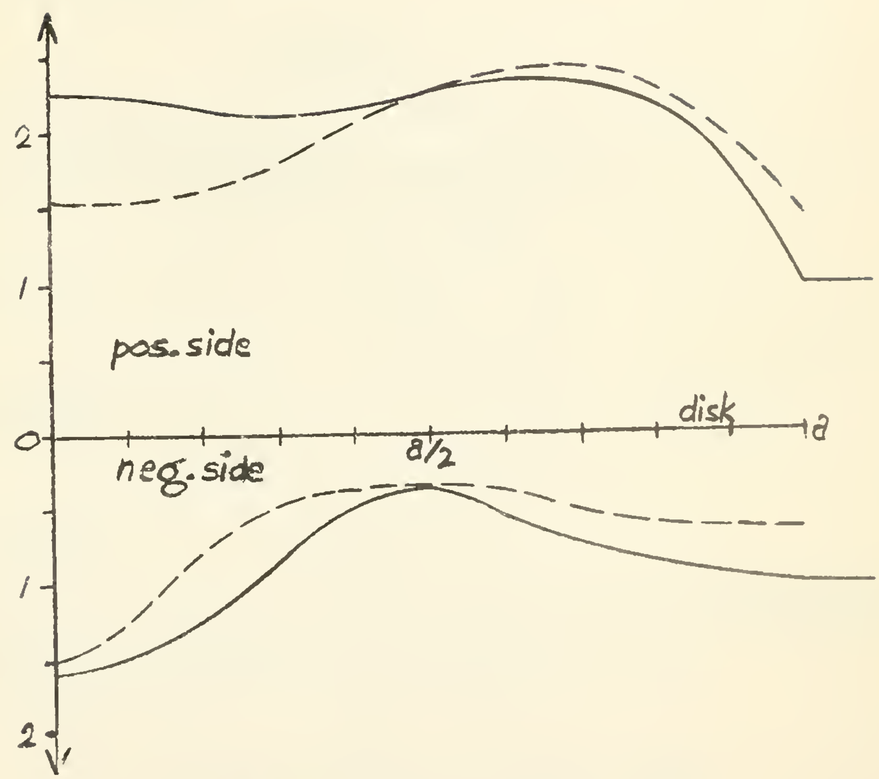

Figure 12

Acknowledgments

The author wishes to express his thanks to Dr. R. D. Spence for his continued encouragement and assistance; to Dr. F. M. Wiener and the Bell Telephone Laboratories for permission to reproduce the experimental data; Drs. Eugene Isaacson, Wiener and the members of the Mathematics Research Group, Washington Square College for many enlightening discussions. A large amount of the computations was performed by Mr. H. B. Keller.

References

1. A. Sommerfeld, Math. Ann. 45, 263 (1894); 47, 317 (1896).
2. J. Schwinger, Fourier Transform of Integral Equations, Lecture Notes.
3. H. Levine and J. Schwinger, Phys.Rev. 73, 383, (1948).
4. J. F. Carlson and A. E. Heins, Qu.Appl.Math., 4, 313 (1947); Heins and Carlson, ibid., 5, 82 (1947); Heins, ibid., 6, 157 and 215 (1948).
5. See for instance J. A. Stratton, Electromagnetic Theory (McGraw-Hill, 1941) pp. 392-409, 414-415).
6. Stratton loc.cit., pp. 563-573; note also remarks on bottom of page 414.
7. H. P. Robertson, Math. Ann. 98, 749(1927), L. P. Eisenhart, Ann.,Math. 35, 284 (1934).
8. J. A. Stratton, P.M.Morse, L.J.Chu and R.A. Hutner, Elliptic Cylinder and Spheroidal Wave Functions (Wiley, 1941), pp. 69-72, 107-127.
9. A. Leitner and R. D. Spence, to be published elsewhere.
10. Epstein, Diss., Munich.
11. P.M.Morse and P. Rubinstein, Phys. Rev. 54, 895 (1938).
12. L.Page, Phys. Rev. 65, 111 (1944).
13. R.M.Ryder, J.Appl. Physics 13, 327 (1942).
14. R.D. Spence, J. Acoust.Soc.Am. 20, 380, (1948).
15. C.J.Bouwkamp, Diss.,Groningen (1941)
16. Rayleigh, Phil. Mag (5), 43, 259, (1897).
17. H. Levine and J. Schwinger, Phys. Rev. 74, 958 (1948).

18. B. B. Baker and E. T. Copson, The Mathematical Theory of Huygens' Principle (Oxford, 1939), pp. 68-72.

19. Baker and Copson, Loc. cit., p. 24.

20. H. Primakoff, M. J. Klein, J.B.Keller and E.L.Carstensen, J.Acous.Soc. Am. 19, 132 (1947).

21. F. M. Wiener, J. Acous.Soc.Am. 19, 444 (1947)

22. F. M. Wiener J. Acous.Soc.Am., 21, 39 (1949; Letter to the Editor); additional material in process of publication; used by permission.

23. See for instance H. Lamb, Hydrodynamics (Dover Reprint 1945), p. 500. An argument leading to the same result and using Green's function is indicated on pp. 13-14 of our paper.

24. See P. M. Morse and H. Feshbach, Methods of Theoretical Physics, mimeographed notes (M.I.T., Technology Press, 1946), p. 349, equation (1.39).

25. Morse and Feshbach, loc.cit., p.155, ff.

26. L. Page, Phys. Rev. 65, 98 (1944)

27. E. G. C. Poole, J. Pure and Appl. Math. 49, 309 (1923).

Date Due

JUL 8 '63			